Inelastic neutron scattering investigation of external modes in incommensurate and commensurate A_2BX_4 materials

1992 J. Phys.: Condens. Matter 4 8551

(http://iopscience.iop.org/0953-8984/4/44/016)

J. Phys.: Condens. Matter 4 (1992) 8551–8564. Printed in the UK

Inelastic neutron scattering investigation of external modes in incommensurate and commensurate A_2BX_4 materials

I Etxebarria†, M Quilichini‡, J M Perez-Mato†, P Boutrouille‡, F J Zúñiga† and T Breczewski†§

† Departamento de Física de la Materia Condensada, Facultad de Ciencias, Universidad del Pais Vasco, Apartado 644, Bilbao, Spain

‡ Laboratoire Léon Brillouin, CEN-Saclay, 91191 Gif-sur-Yvette Cédex, France

Received 1 April 1992, in final form 8 July 1992

Abstract. Inelastic neutron scattering experiments in K_2SeO_4, Cs_2SeO_4 and K_2CrO_4 are reported. The lowest Σ_3–Σ_2 phonon branches along the a^*-axis in their *Pnam* phase have been characterized for the three compounds. The results are compared with recent lattice dynamical simulations using rigid-ion models. Potassium chromate, that simulations suggested to be incommensurate at low temperatures, evidences no structural phase transition down to 12 K, but its lowest Σ_2 phonon branch exhibits a significative softening and decreases more than 20% as the temperature is lowered from 300 K to 36 K. The softening mechanism in this compound and in potassium selenate is related to an increase of the effective interaction between an acoustic and an optical branch.

1. Introduction

Many materials of the type A_2BX_4, isomorphous with β-K_2SO_4 (space group *Pnam*), transform at lower temperatures into an incommensurately modulated (INC) phase with the modulation wavevector along the a-axis. The symmetry of the distorting mode (order parameter) is Σ_2 (antisymmetric for the a and m symmetry planes). If the temperature is further decreased, a second phase transition into a commensurate phase takes place and the modulation wavevector locks into a commensurate value, which is $\frac{1}{3}a^*$ in many materials. This general scheme is reproduced in most of the compounds, but particular features vary considerably. The compounds of Zn (Rb_2ZnCl_4, Rb_2ZnBr_4 and K_2ZnCl_4) do not exhibit a proper soft-phonon mode, and the tetrahedral groups BX_4 seem to be disordered in two equivalent positions in the *Pnam* normal phase [1]. In contrast, a clear Σ_2 soft mode has been observed in K_2SeO_4 [2], and for this compound x-ray structural analyses of the normal phase have been successful using non-disordered models [3, 4]. For a general review see [5, 6].

The microscopic mechanism of the incommensurate structural instability in A_2BX_4 compounds has been investigated by studying the lattice dynamics of rigid-ion models [7–14]. In particular, very simplified empirical models with the BX_4 groups approximated as rigid units are quite successful in reproducing the essential features of the experimental data [13–15]. A force model with only three adjustable parameters,

§ On leave of absence from the Institute of Physics, A Mickiewicz University, Poznan, Poland.

0953-8984/92/448551+14$07.50

only optimized to be consistent with the *static* structural data in the *Pnam* phase, is sufficient to reproduce the basic features of the incommensurate structural instability [14, 15]. In particular, the model predicts an unstable or soft mode with characteristics analogous to the experimental ones, and shows that the effective size of the cations in comparison with the size of the tetrahedral BX_4 groups is a fundamental factor for the mechanism of the structural transition; in broad terms, smaller distances A–X or a smaller effective size of the cations A, in comparison with the size of the anionic groups, tend to make the *Pnam* structure unstable with respect to an incommensurate modulation. In addition, the distribution of charge within the BX_4 groups has a smaller but noticeable influence: smaller values of the effective charge of ion B tend to stabilize the *Pnam* structure. The energetic and lattice dynamics calculations within this simple empirical model could predict the qualitative differences of the incommensurate transition between potassium selenate and the Zn compounds and the absence of an incommensurate instability in isostructural compounds such as K_2SO_4, Rb_2SeO_4, Cs_2SeO_4, Cs_2ZnCl_4 and Cs_2ZnBr_4. In those compounds having an incommensurate instability, an unstable Σ_2 phonon branch was obtained and a multiple well structure associated to modulated configurations of lower energy than the *Pnam* structure was observed in the potential energy surface. A quantitative analysis of the potential energy surfaces for the different compounds within a simplified one-dimensional model led to an estimation of their transition temperatures, which is in close agreement with the experimental values. In the case of those compounds known to be stable in the *Pnam* phase down to low temperatures, the phonon branches were all stable, indicating that the *Pnam* configuration is an actual minimum of the potential energy surface in configuration space. Indeed, for some of these compounds, a small decrease of the lattice energy for a Σ_2 distortion could be detected, but considering the roughness of the model, this decrease was not significant compared with those obtained in compounds with modulated phases. However, in the case of K_2CrO_4, the calculated dispersion curves included an unstable Σ_2 phonon branch with qualitative and quantitative features similar to those obtained for the prototypic incommensurate material K_2SeO_4. In general the whole structure of the calculated low-frequency dispersion curves was very similar and could be explained by the similarity of the effective sizes of the selenate and chromate groups. On the other hand, the calculated depth for the energy well corresponding to the Σ_2 distortion in potassium chromate was four times smaller than in potassium selenate. Despite this important difference, a simplified one-dimensional energetic model suggested for potassium chromate a structural instability in the range 30–70 K. This compound was therefore considered as a potential incommensurate material at low temperatures.

An important result of the lattice dynamics calculations in [13–15] is that in all cases the unstable phonon branch was either optical or the result of the anticrossing of an optical branch with an acoustic one. The real instability mechanism seemed therefore to be quite different from that suggested by one-dimensional models which consider only the degrees of freedom of a single acoustic branch [2].

Previous inelastic neutron scattering investigations in A_2BX_4 materials have focused on the temperature behaviour of the soft-mode branch and the characterization of phason and amplitudon branches in the INC phase [2, 16–20]. Here we report inelastic neutron scattering measurements of the low frequency Σ_3–Σ_2 modes (same notation for irreducible representations as in [2]) of K_2SeO_4, Cs_2SeO_4 and K_2CrO_4 in the *Pnam* phase. The main purpose of the study has

been to obtain a minimal comparative characterization of the low-frequency phonon branches corresponding to external modes, in which the role of the internal degrees of freedom of the BX_4 tetrahedra can be neglected. The results are compared with the predictions of model calculations for the different compounds and a simple phenomenological model is proposed for the role of the anticrossing of the acoustic and optical branches in the phonon softening. Also, the eventual existence at low temperatures of an incommensurate structural instability and soft mode in potassium chromate has been investigated.

2. Experimental method

Single crystals of K_2SeO_4, Cs_2SeO_4 and K_2CrO_4 were grown isothermally at 310 K from aqueous solution by a dynamic method. The samples were of good quality with an average volume of 0.5 cm^3 and approximate mosaic spread of 20′. They were mounted in an aluminium can filled with He gas and placed in a displex closed cycle cryostat. Data were taken as a function of temperature with a 0.05 K stability. Inelastic neutron scattering measurements have been performed on a three-axis spectrometer located on a cold source at the Orphée Reactor (LLB-CEN-Saclay, France). Constant $k_i = 2.662$ Å^{-1} or 1.64 Å^{-1} scans allowed us to measure phonons in neutron energy gain with a flat analyser. Both monochromator (vertically bent) and analyser were of pyrolytic graphite (PG[002]). A pyrolytic graphite filter was used on incident k_i to avoid second-order contamination. Horizontal collimations on incoming and outcoming neutrons were such that for most of the data the energy resolution was (for null energy transfer) 0.3 THz and 0.07 THz at $k_i = 2.662$ Å^{-1} and 1.64 Å^{-1}, respectively.

The modes propagating along the a^*-axis of symmetry Σ_3–Σ_2 are mainly transversal with most atomic displacements restricted along the c-axis. In order to measure the corresponding dispersion curves, the samples were oriented with a scattering plane defined by a^* and c^*. The Brillouin zones investigated were essentially those centred at the reciprocal lattice points (0,0,4), (1,0,4), (2,0,4), (0,0,5) and (1,0,5). Because of the symmetry, the phonon branches along the a^*-axis are degenerate by pairs (Σ_3,Σ_2) and (Σ_4,Σ_1) at $q = a^*/2$, and their pattern corresponds to an effective cell parameter $a/2$ along the a-axis. It is, therefore, convenient to represent the dispersion curves in an extended Brillouin zone scheme, where a pair of branches Σ_3–Σ_2 constitutes a single dispersion curve. Furthermore, the one-phonon scattering cross section of the modes follows in general an intensity pattern consistent with this scheme, so that the phonon symmetry assignment can be done directly considering the Brillouin zone in which the mode has been detected. Accordingly, the results have been plotted so that the wavevectors for the Σ_3 and Σ_2 branches are in the range 0–0.5a^* and 0.5–1a^*, respectively. The transverse Σ_3 acoustic mode was detected near the strong (0,0,4) Bragg reflection for $q \leqslant a^*/2$, whereas for $a^*/2 \leqslant q \leqslant a^*$ the lowest Σ_2 branch has been measured at best in the $(1+\xi,0,4)$ zone with $0 \leqslant \xi \leqslant 0.5$.

Molecular dynamics (MD) simulations [21] of the neutron structure factor for potassium selenate using the force model in [15] suggested that optical Σ_3 branches would be easier to detect in the (0,0,5) Brillouin zone rather than in the (0,0,4) zone (see figure 1(c)). This was confirmed by experiment and consequently, data mostly obtained at the (0,0,5) Brillouin zone have been employed to construct the Σ_3 part

of the dispersion curves in this compound. Finally, the fourth branch in potassium selenate was observed only in the zones (0,0,5) and (1,0,5). The ability of the empirical force model to predict correct intensity features in the neutron scattering spectrum is clearly demonstrated in figure 1 where the experimental spectra at the points (0,0,4) and (0,0,5) are compared with the corresponding structure factors obtained from MD simulations. Although the positions of the simulated peaks are displaced with respect to the experiment, their intensity structure is well reproduced.

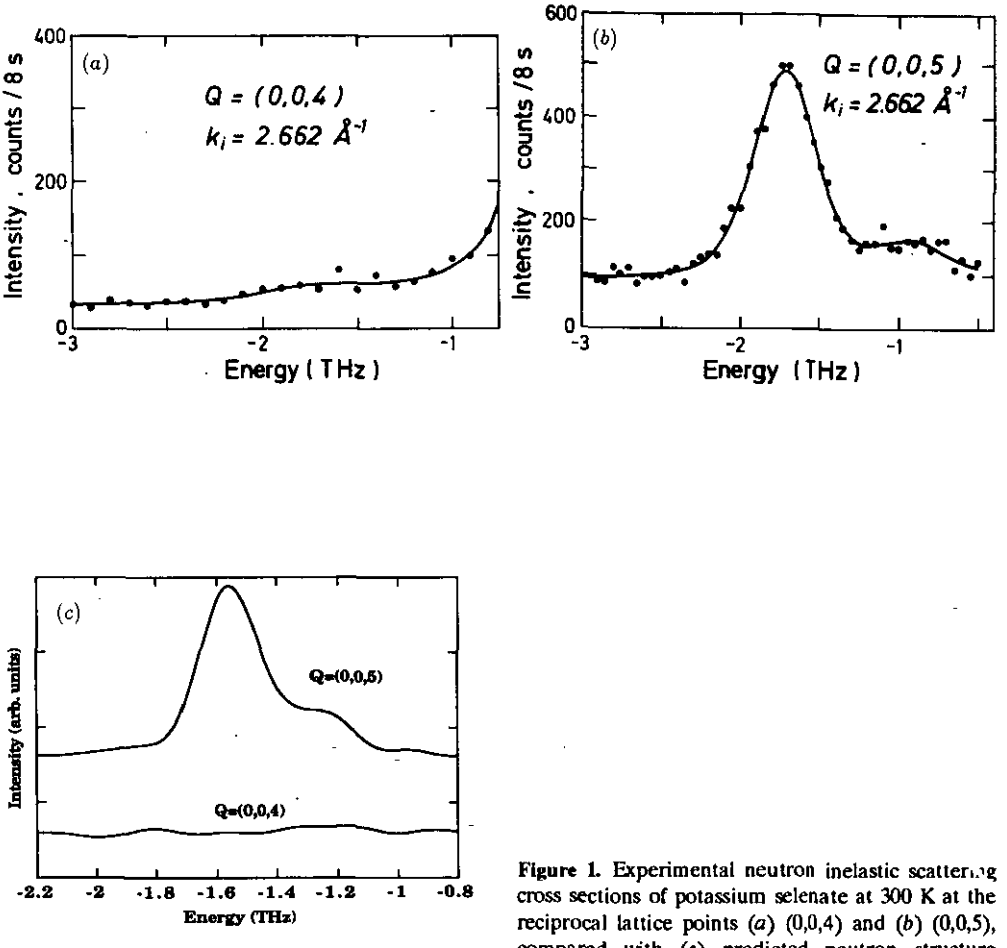

Figure 1. Experimental neutron inelastic scattering cross sections of potassium selenate at 300 K at the reciprocal lattice points (*a*) (0,0,4) and (*b*) (0,0,5), compared with (*c*) predicted neutron structure factors obtained by means of molecular dynamics simulations using the force model mentioned in the text.

In the case of Cs_2SeO_4, the temperature dependence of the lowest Σ_2 branch was also investigated. Measurements at 100 K and 50 K were performed showing that the branch is temperature independent. For potassium chromate the (0,0,5) zone could not be reached with incident neutrons of wavevector $k_i = 2.662$ Å^{-1}; we

have therefore measured only the lowest Σ_3–Σ_2 branches in the (0,0,4) and (1,0,4) zones. Our experimental study of this compound was specially devoted to measuring its temperature behaviour as shown in figure 4(*a*) and discussed below.

All our data were systematically fitted taking into account resolution effects. This was achieved by computing the convolution of the response function (described by a damped harmonic oscillator function) with the resolution function of the spectrometer. Least-square refinements with the raw data give the inelastic structure factor, the quasiharmonic frequency and the damping of the measured mode. In particular this allows us to have a precise picture of the q-dependence of the structure factor of each mode, which helps to evidence the observed anticrossing between modes discussed in the following section.

3. Results and discussion

The phonon frequencies for the lower Σ_3–Σ_2 branches of K_2SeO_4, Cs_2SeO_4 and K_2CrO_4 at 300 K, obtained as indicated in section 2, are plotted in figures 2(*a*), 3(*a*) and 4(*a*), respectively.

3.1. K_2SeO_4

A comparison of the dispersion curves of potassium selenate in figure 2(*a*) with the data at 250 K reported in [2] for the two lowest curves indicates that the soft-phonon Σ_2 branch already suffers a considerable general decrease in the temperature interval 300–250 K; for instance, in figure 2(*a*) the minimum of the branch is situated at the border of the extended Brillouin zone, with no indication of the softening centred around $0.7a^*$ which is already obvious at 250 K [2]. On the other hand, the slightly higher values obtained in the present experiment for the second branch in the range 0.2–$0.5a^*$ (Σ_3 symmetry) cannot be attributed to the different temperatures investigated, since we could observe that as temperature is lowered from 300 K to 160 K this second branch clearly hardens around the point $0.3a^*$.

The essential features of the dynamical softening mechanism predicted by the lattice dynamics simulations are confirmed in figure 2(*a*). The four lowest calculated Σ_3–Σ_2 phonon branches are reproduced in figure 2(*b*). In the same figure we also plot the thermal effective frequencies at $q = 0$, $\frac{1}{3}$, $\frac{2}{3}$ and $1a^*$ for the two lowest Σ_3–Σ_2 branches, obtained in a recent MD study at 250 K using the same force model [21]. The results of the MD simulations show the strong thermal renormalization of the lowest branch of the force model, which is enough to stabilize the *Pnam* phase. The experimental sound velocity is in excellent agreement with the calculated one, while, as predicted by the MD simulations, the observed anticrossing of the first two branches takes place at values of q larger than in the mechanical model. This can be explained by the thermal renormalization of the unstable branch, which, as observed in the simulations, raises the whole branch to stable values and displaces the effective anticrossing of the two branches to higher wavevectors. The form of the experimental second branch in the range 0.3–0.7 agrees closely with what could be expected from the MD results and the lattice dynamical model, while the results at the Brillouin zone centre (both $q = 0$ and $1a^*$) show important discrepancies.

Although the third and fourth branches in figure 2(*b*) have a similar structure to those measured, they are systematically lower than the experimental ones. The thermal increase of the frequencies due to anharmonic effects observed in the MD

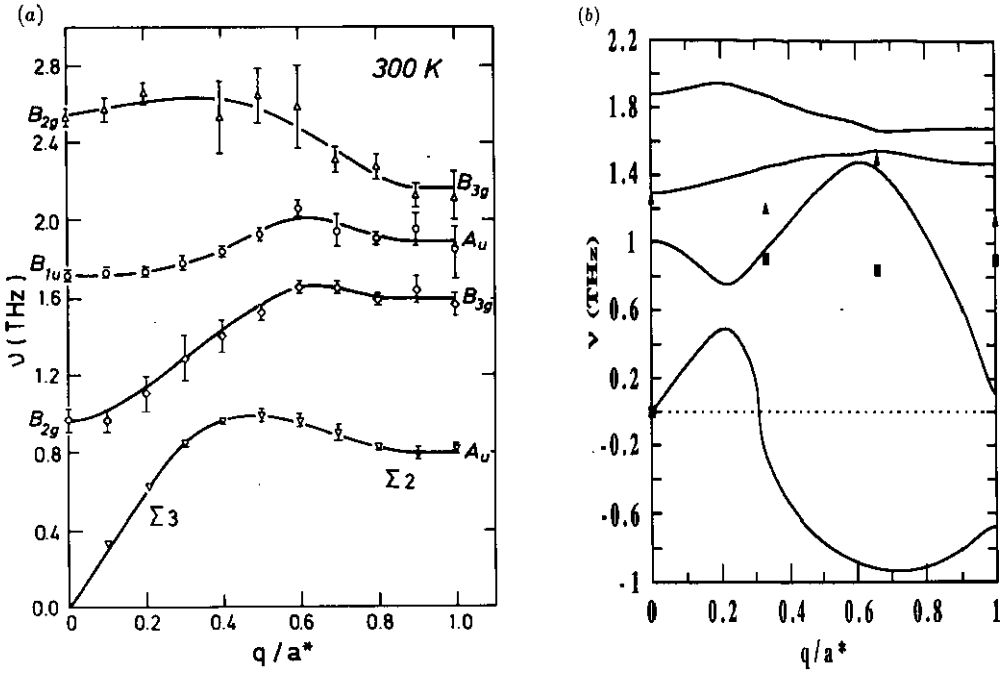

Figure 2. (*a*) Experimental low frequency Σ_3–Σ_2 phonon dispersion curves at 300 K of potassium selenate in an extended zone scheme; (*b*) lowest Σ_3–Σ_2 phonon dispersion curves of the same compound calculated according to the model mentioned in the text [15]. The squares and triangles in (*b*) correspond to the points of the acoustic and lowest transverse optical branch obtained from molecular dynamics simulations at 250 K using the same force model.

simulations for these branches is not larger than 0.3 THz, much lower than the difference of 0.6 THz observed for instance in the fourth branch. However, the most conspicuous discrepancy between the experiment and the simulations is the behaviour of the second branch in the range 0.7–1a^* (Σ_2-symmetry). In the calculations, the instability of the first branch is accompanied by a very steep decrease of the second branch in this range. According to MD simulations, as thermal effects raise the unstable branch to stable values around the experimental ones, the second branch in the interval 0.7–1a^* is also 'pushed' to much higher values than those given by the mechanical model (see figure 2(*b*)). In the experiment, however, the second branch has at $q = 1a^*$ an even higher value than predicted by MD, and is at 300 K nearly horizontal in the range 0.6–1a^*. We observed by measuring the phonon spectrum at 161 K and 131 K at the point (1,0,4) that the second branch decreases by about 10% (0.17 THz) in the interval 300–131 K, while the softening of the first branch at this point in the same temperature interval is 37% (0.3 THz). Hence, the second Σ_2 branch evidences important thermal renormalization effects having a close link with the softening of the first branch that are consistent with the model, but they are weaker than expected from the MD simulations [21].

Irreducible representations Σ_3 and Σ_2 are compatible at the Brillouin zone centre with B_{2g} (xz) or B_{1u} (z), and B_{3g} (yz) or A_u, respectively. Hence, in figure 2 these are the symmetries of the modes at $q = 0$ and $q = 1a^*$. Several Raman and infrared studies of potassium selenate have been published in recent years [22–27] that can be

compared with the results of figure 2(*a*). Many optical modes are expected in the low-frequency range (over ten with a frequency lower than 3 THz); hence, experimental data (Raman and IR) are rather complex. As a consequence, several inconsistencies between the different authors can be detected. At room temperature most of the modes are not completely resolved and, moreover, modes which belong to different symmetry species appear to be degenerate in energy. At lower temperatures, modes become more resolved and some degeneracies are removed. After a careful inspection of published results, taking into account the different settings used in the literature, and after having discarded those data suspected of spurious contamination due to imperfect polarization of the light, most of the apparent discrepancies between the different authors can be solved, and a proper comparison with the present neutron experiments could be performed. The second optical branch at the $q = 0$ corresponds to a polar mode B_{1u} measured at 1.8 THz in [25, 26] and the third optical branch at $q = 0$ can be assigned to the B_{2g} ((ac) geometry) mode detected at 2.42 THz in [28, 29] and at 2.25 THz in other works. An additional B_{2g} mode at 1.5–1.6 THz reported by some authors [24, 25] is not consistent with the neutron results in figure 2(*a*). At $q = 1a^*$ the first optical mode can be assigned to the strong B_{3g} ((bc) geometry) mode observed at 1.57 THz in [22, 28, 29], while the weak B_{3g} mode at 2.25 THz [22, 25, 28] can be identified with the end of the fourth branch. Only the first optical branch at $q = 0$ is difficult to assign; we propose to identify it with a weak Raman B_{2g} mode of 1 THz reported in [28]. According to these results, the end of the soft-phonon branch at $q = 1a^*$ can be confirmed as an optical silent A_u mode.

3.2. Cs_2SeO_4

In this compound, as expected from the simulations (see figure 3(*b*)), the anticrossing between the acoustic and the first optical branch is displaced to larger wavevectors because of the smaller slope of the acoustic branch. In fact, the anticrossing is not fully realized before reaching the zone boundary. As a consequence, the characteristic scheme of the softening of potassium selenate does not exist. Although the first optical branch has at $q = 0.3a^*$ even lower values than in potassium selenate, the absence of any potential instability is indicated by the clear tendency of the branch to higher frequency values as the wavevector increases. At $q = 1a^*$ the lower branch is in the range 1.1–1.2 THz, in contrast with potassium selenate, which despite the smaller mass of potassium, does not reach more than 0.8 THz. As mentioned in section 2, the phonon branches depicted in figure 3(*a*) were also measured at 100 K and 50 K and no significant temperature dependence was detected. The general structure of the four measured branches follows quite closely the model scheme of figure 3(*b*). However, the frequencies are in general larger than those obtained in the simulations, specially in the case of the third and fourth branches, where the differences reach values of the order of 0.7 THz. The sound velocity that can be deduced from the measured dispersion branch (1672 m s^{-1}) is also about 8% larger than the one derived from the force model. The shortcomings in the force model giving rise to these discrepancies could be related to the charges assigned to the different ions. It was suggested in [30] that the effective charge of the selenate groups may not reach the nominal value of $-2e$; this possible cause, however, can be discarded since force models where the effective charge for cesium atoms is fixed to smaller values than $1e$ give place to phonon spectra of even lower frequencies than those in figure 3(*b*). On the other hand, a redistribution of the effective charge within the tetrahedral selenate groups, keeping $-2e$ as the net charge, can produce

significant changes. We calculated, for instance, the lowest four Σ_3–Σ_2 branches using a force model optimized for cesium selenate in the form described in [14, 15], but with the charge of Se fixed to $1e$, instead of the adjusted value $1.33e$ used for figure 3(*b*); the optical branches rise considerably, the branch structure is more similar to the experimental result, the first optical branch being now at a range comparable with the experimental one, but the second and third optical branches are still too low. As in the case of potassium selenate, a more accurate dynamic prediction would require the introduction of more complex force models. Nevertheless, it is clear from the present results that the mechanism of the incommensurate instability involves in practical terms only the first two branches, and a rigid-ion model is enough to put in evidence the essential differences observed between potassium and cesium selenate with respect to these degrees of freedom.

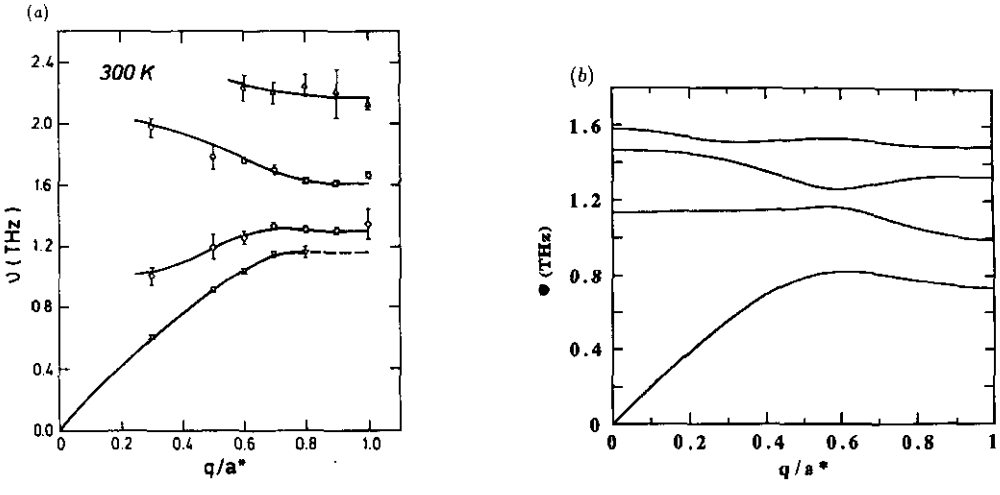

Figure 3. (*a*) Experimental low frequency Σ_3–Σ_2 phonon dispersion curves at 300 K of cesium selenate in an extended zone scheme; (*b*) lowest Σ_3–Σ_2 phonon dispersion curves of the same compound calculated according to the force model mentioned in the text [15].

Measurements of Raman frequencies for cesium selenate in the range 20–650 K have been reported in [30]. The *Pnam* structure was shown to be stable down to low temperatures, in accordance with the simulations. Comparing figure 3(*a*) with the results in [30], the ends of the second and fourth branches at $q = 1a^*$ can be identified as B_{3g}, while the others must be Raman silent (A_u). On the other hand, the lowest B_{2g} frequencies reported in [27] (B_{1g} in their notation) are not easy to reconcile with the neutron results of figure 3(*a*).

3.3. K_2CrO_4

According to figure 4(*a*), potassium chromate can be considered as an intermediate case between the two compounds studied above. The first optical branch has in the range 0.5–$1a^*$ similar values to those of cesium selenate, but the anticrossing with the acoustic branch is in this case fully realized because of the higher sound velocity

in potassium chromate. The hybridization between the two branches takes place in the range 0.4–0.6a^*, while in potassium selenate it is in the region 0.3–0.5a^*. This displacement is due to the higher values of the first optical branch, while the acoustic branch, in accordance with the simulations, has a similar slope in both compounds (see figures 2(*b*) and 4(*b*)).

The incommensurate structural instability suggested by the model calculations shown in figure 4(*b*) was checked by means of a systematic search of satellite reflections at low temperatures. Down to 12 K no evidence of a phase transition was detected. Neutron powder diffraction diagrams have also confirmed that no phase transition occurs down to 2 K. However, measurements of the Σ_2 phonon branches at 66 K and 36 K showed, in contrast with the measurements in cesium selenate, a clear softening of the lowest branch. The results at 36 K are shown in figure 4(*a*). As the data points for the second branch coincide within experimental resolution with those obtained at 300 K, only those corresponding to the lowest branch are plotted. The conspicuous decrease of the single branch follows, as suggested by the simulations, the same pattern observed in potassium selenate. The softening, however, starts from higher values than in this latter compound and only reaches in the temperature interval 300–36 K a decrease of the order of 20%. The lowering takes place along the whole branch, keeping its flat structure, similar to potassium selenate in figure 2(*a*), where no minimum outside the Brillouin zone boundary can be seen.

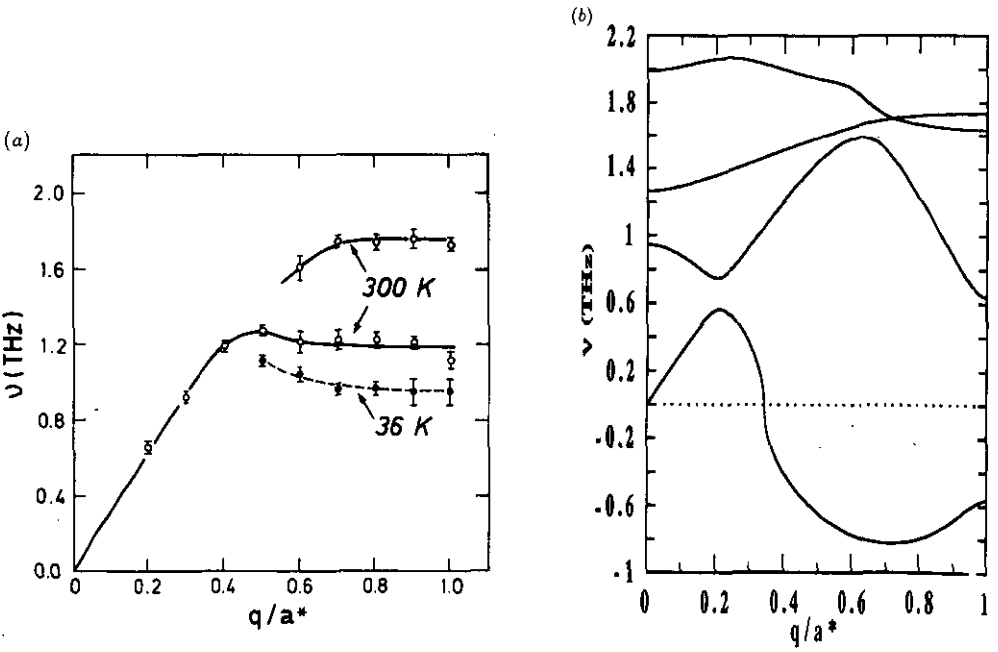

Figure 4. (*a*) Experimental low frequency Σ_3–Σ_2 phonon dispersion curves at 300 K and 36 K of potassium chromate in an extended zone scheme; only significant temperature variations are indicated which are limited to the lowest Σ_2 branch; (*b*) lowest Σ_3–Σ_2 phonon dispersion curves of the same compound calculated according to the force model mentioned in the text [15].

As happened with potassium selenate, the force model introduces in the range 0.7–1a^* a strong structure for the second branch, which is hardly compatible with the experimental results; the theoretical second branch has a strong negative slope

and can be considered the prolongation after several anticrossing of a branch starting at $q = 0$ at much higher frequencies. On the other hand, in the real material this branch, if existent, does not reach such low values at the border of the Brillouin zone.

3.4. Phenomenological model of the mode softening

A simple mechanism for the soft-mode behaviour observed in potassium selenate was proposed in [2] and has been widely diffused [5, 6, 31]. The lowest Σ_3–Σ_2 branch, having an acoustic character around the Brillouin zone centre, was described in terms of a local mode model with a single translationally invariant local degree of freedom; thus, the phonon branch could be interpreted as that of a one-dimensional 'monoatomic' chain with unit cell $a/2$. The branch softening was then related to the increase at low temperatures of third-neighbour interactions and the simultaneous decrease of second- and first-neighbour ones, so that at the transition temperature the values of this latter were much smaller (or negative) compared with those between third neighbours. The results of figure 2(*a*) show, however, that such a model puts aside an important feature of the phonon spectrum of the system, that was already anticipated by rigid-ion simulations. It can be seen that there exists a clear complete anticrossing of the acoustic and the first optical branch of Σ_3–Σ_2 symmetry, in such a way that the lowest Σ_2 branch can be considered the natural prolongation of the first optical branch. We believe that this in fact invalidates any model that oversimplifies the system to a single phonon branch. The actual mechanism seems to have many more similitudes to the basic model proposed by Axe *et al* [32] and developed by Vallade *et al* and others [33–35] for the particular case of quartz. In this model a soft optical branch with its minimum at the Brillouin zone centre, interacts with an acoustic branch of the same symmetry and gives place as it lowers down with temperature to a local minimum out of the zone centre which gives place to the incommensurate instability. It is important to stress that, in such a scheme, temperature effects were introduced through the assumption of a thermal softening of the optical branch as a whole.

Three important points distinguish the case of potassium selenate when transposed into this model: (i) the optical branch is rather flat and high; (ii) as a consequence, the interaction of both branches is essentially located in a region of wavevectors quite distant from the zone centre, and (iii) the optical branch at the zone centre (Raman active) is temperature independent [29]. The interaction between both branches and its temperature behaviour is therefore quite different from that in quartz. Nevertheless, we can develop a similar simple model.

Let us consider a flat optical branch, $\omega_0^2(q) = \text{constant}$, and a typical acoustic branch, $\omega_A^2(q) = A\sin^2(\pi q/2)$, where q is defined by the relation $q = qa^*$. The two branches, being of the same symmetry, interact through a coupling term $V(q)$, such that the actual normal frequencies of the system are given (see figure 5) by the eigenvalues of the matrix

$$\begin{pmatrix} \omega_0^2(q) & V(q) \\ V(q) & \omega_A^2(q) \end{pmatrix}. \tag{1}$$

In the limit of null wavevector, both branches should be uncoupled and $V(q)$ goes to zero as q^2. In the case of potassium selenate, as the interaction is not restricted to small wavevectors, we cannot restrict the form of $V(q)$ to this limit, and a general

expression for $V(q)$ should be considered:

$$V(q) = \sum_n C_n \sin^2(n\pi q/2). \tag{2}$$

In figure 5, it can be seen how an interaction of the type (2), with a single first-order term results in a phonon branch scheme similar to the one observed in potassium selenate at room temperature (see figure 2(*a*)). Of course, in the experimental case, the whole picture becomes more complicated by additional anticrossings of the acoustic branch with optical branches of higher frequencies, but these additional degrees of freedom do not play an essential role in the low frequency region and are disregarded here. It is also shown in figure 5 how a small second-order interaction ($C_2 \neq 0$) is enough for introducing in the lowest branch a clear minimum centred around $\frac{2}{3}$, similar to the one observed at low temperatures in potassium selenate [2]. It should be stressed that in this simulation, the value attributed to the second-order interaction is much smaller than the one given to the first-order term, and that the conspicuous minimum of the branch is strongly dependent on the value of C_2, a slight increase with respect to the value used in the figure is sufficient to make the branch unstable.

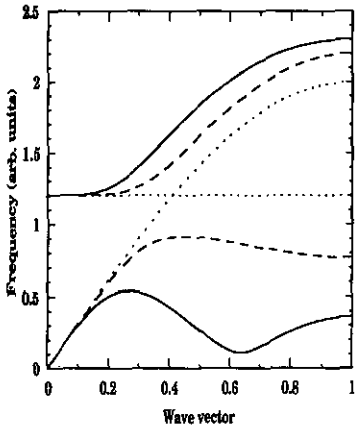

Figure 5. Phonon dispersion curves resulting from different interactions between an acoustic and an optical branch as explained in the text. The dotted, dashed and solid lines correspond to the non-interacting scheme ($\omega_0 = 1.2$, $A = 1.0$, $C_1 = C_2 = 0$), first-neighbour interactions ($\omega_0 = 1.2$, $A = 4.0$, $C_1 = 1.7$, $C_2 = 0$), and first- and second-neighbour interactions ($\omega_0 = 1.2$, $A = 4.0$, $C_1 = 2.25$, $C_2 = 0.5$), respectively.

The interaction constants C_n in (2) can be given a simple microscopic meaning; if we call y_i the local coordinates corresponding to the bare optical branch and x_i the local translational degreees of freedom associated with the bare acoustic branch, the potential energy can be written as

$$V = \sum_i \tfrac{1}{2}\omega_0^2 y_i^2 + \tfrac{1}{8}A(x_i - x_{i+1})^2 + W(x, y) \tag{3}$$

where $W(x, y)$ is a coupling term between both sets of coordinates. The most general form of the first-neighbour interaction, maintaining the modes x, y uncoupled at $q = 0$, is

$$W_1(x, y) = \tfrac{1}{4}C_1' \sum_i (y_i - y_{i-1})(x_i - x_{i-1}). \tag{4}$$

When translated into Fourier space this interaction contributes to a first-order term in (2). Analogously, the second term in expression (2) can be related, for instance, to second-neighbour interactions of the form:

$$\tfrac{1}{4}C_2 \sum_i (y_i - y_{i-2})(x_i - x_{i-1}) + (y_i - y_{i-1})(x_i - x_{i-2}). \tag{5}$$

Hence, a mode softening similar to that observed in potassium selenate is simulated by means of a one-dimensional model with two local degrees of freedom, one being of acoustic character. This supports microscopic approaches as those proposed in [36, 37] where the thermodynamics of A_2BX_4 systems is analysed considering two local modes. In contrast to the phenomenological model proposed for quartz we are able to reproduce thermal effects by assuming a temperature dependence of the effective interaction among the modes up to second neighbours. In particular, the branch softening around $\frac{2}{3}a^*$ at low temperatures is essentially caused by an increase of the effective second-neighbour interactions. This is in accordance with the point stressed by Janssen [37] that second-neighbour interactions are essential for having an incommensurate phase in models with two local modes. It should be stressed that although the mode softening is essentially reproduced by means of an increase of second-neighbour effective interactions, these latter keep in the simulation, up to the incommensurate instability, a reasonable ratio with the value of first-neighbour interactions.

If this picture of the structural instability is essentially correct, it is expected that as temperature is lowered and the softening builds up in the lowest branch, the first optical branch slightly hardens at the anticrossing region, contributing to the gap increase between both branches. We could confirm this behaviour by comparing the phonon spectrum of potassium selenate at the point (0.3,0,5) at 300, 200 and 160 K. In the temperature interval 300–160 K the second branch at this point increased its value in about 0.2 THz, while the phonons corresponding to the soft branch decrease their frequency in less than 0.1 THz and the third branch is essentially temperature independent.

4. Conclusions

As expected from rigid-ion model calculations, potassium chromate exhibits a thermal softening of its lowest Σ_2 phonon branch. The softening is, however, incomplete and the *Pnam* phase is stable up to low temperatures.

The lowest Σ_3–Σ_2 phonon branches in potassium selenate and cesium selenate have a structure which qualitatively agrees with the results of model lattice dynamics calculations and molecular dynamics simulations. In particular, the present work confirms the essential role played by the interaction between the first optical Σ_3–Σ_2 branch and the acoustic branch of the same symmetry in the mode softening

observed in potassium selenate. This softening can be explained as the result of a temperature-dependent coupling between both branches. Phenomenological models which only consider a single local translational degree of freedom to describe the soft-phonon branch do not consider this essential feature of the instability and may lead to unphysical conclusions.

Acknowledgments

We gratefully acknowledge the collaboration of G André, who performed the neutron powder diffraction test of potassium chromate mentioned in the text. Two of the authors (IE and JMPM) want also to express their gratitude for the hospitality of the 'groupe inelastique' of the LLB during the realization of the present work. Thanks are also due from one of the authors (IE) to the Spanish Ministry of Education and Science (Dirección General de Investigación Científica y Técnica) for its financial support. This work was also partially supported by the Universidad del Pais Vasco (Project UPV 063.310-E180/90).

References

[1] Itoh K, Hinasada A, Matsunaga H and Nakamura E 1983 *J. Phys. Soc. Japan* **52** 664
[2] Iizumi M, Axe J D, Shirane G and Shimaoka K 1977 *Phys. Rev.* B **15** 4392
[3] Kalman A, Stephens J S and Cruickshank D W J 1970 *Acta Crystallogr.* B **26** 1451
[4] Yamada N and Ikeda T 1984 *J. Phys. Soc. Japan* **53** 2555
[5] Axe D, Iizumi M and Shirane G 1986 *Incommensurate Phases in Dielectrics. Part II, Materials* ed R Blinc and A P Levanyuk (Amsterdam: North-Holland) p 1
[6] Cummins H Z 1990 *Phys. Rep.* **185** 211
[7] Haque M and Hardy J R 1980 *Phys. Rev.* B **21** 245
[8] Katkanant V, Edwarson P J, Hardy J R and Boyer L 1989 *Phase Transit.* **15** 103
[9] Edwarson P J, Katkanant V, Hardy J R and Boyer L 1987 *Phys. Rev.* B **35** 8470
[10] Katkanant V, Edwarson P J, Hardy J R and Boyer L 1986 *Phys. Rev. Lett.* **57** 2033
[11] Lu H M and Hardy J R 1990 *Phys. Rev.* B **42** 8339
[12] Liu D, Lu H M, Ullman F G and Hardy J R 1991 *Phys. Rev.* B **43** 6202
[13] Etxebarria I, Perez-Mato J M and Criado A 1990 *Phys. Rev.* B **42** 8482
[14] Perez-Mato J M, Etxebarria I and Madariaga G 1991 *Phys. Scr.* **T39** 81
[15] Etxebarria I, Perez-Mato J M and Madariaga G *Phys. Rev.* B **46** 2764
[16] Axe J D, Iizumi M and Shirane G 1980 *Phys. Rev.* B **22** 3408
[17] Press W, Majkrzak C F, Axe J D, Hardy J R, Massa N E and Ullman F G 1980 *Phys. Rev.* B **22** 332
[18] Quilichini M and Currat R 1983 *Solid State Commun.* **48** 1011
[19] de Pater C J and van Dijk C 1978 *Phys. Rev.* B **18** 1281
[20] Gesi K and Iizumi M 1984 *Phys. Rev.* B **53** 4271
[21] Etxebarria I, Lynden-Bell M and Perez-Mato J M *Phys. Rev.* B at press
[22] Wada M, Sawada A, Ishibashi Y and Takagi Y 1977 *J. Phys. Soc. Japan* **42** 1229
[23] Massa N E, Ullman F G and Hardy J R 1980 *Ferroelectrics* **25** 601
[24] Massa N E, Ullman F G and Hardy J R 1983 *Phys. Rev.* **27** 1523
[25] Katkanant V, Hardy J R and Ullman F G 1988 *Ferroelectrics* **82** 185
[26] Petzelt J, Kozlov G V, Volkov A A and Ishibashi Y 1979 *Z. Phys.* B **33** 369
[27] Echegut P, Gervais F and Massa N E 1986 *Phys. Rev.* B **34** 278
[28] Fawcett V, Hall R J B, Long D A and Sankaranarayanan V N 1974 *J. Raman Spectrosc.* **2** 629
[29] Quilchini M 1984 unpublished
[30] Ethier L, Massa N E, Beliveau A and Carlone C 1989 *Can. J. Phys.* **67** 657
[31] Aksenov V L, Plakida N M and Stamenkovic S 1989 *Neutron Scattering by Ferroelectrics* (Singapore: World Scientific)

[32] Axe J D, Harada J and Shirane G 1970 *Phys. Rev.* B **1** 1227
[33] Berge B, Dolino G, Vallade M, Boissier M and Vacher R 1984 *J. Phys. C: Solid State Phys.* **45** 715
[34] Berge B, Bachheimer J P, Dolino G, Vallade M and Zeyen C M E 1986 *Ferroelectrics* **66** 73
[35] Tautz F S, Heine V, Dove M T and Chen X 1991 *Physics and Chemistry of Minerals* **18** 326
[36] Chen Z Y and Walker M B 1990 *Phys. Rev. Lett.* **65** 1223
[37] Janssen T 1992 *Z. Phys.* B **86** 277